International Journal of Scientific Research & Engineering Trends
Volume 11, Issue 1, Jan-Feb-2025, ISSN (Online): 2395-566X

Vivaldi Antenna Design for Cognitive Radio Communication

Assistant Professor Dr.K.Jayanthi, B.Loganayaki
Department of Electronics and Communication Engineering, Government College of Engineering, Salem, India

Abstract- This project presents a versatile antenna design suitable for various wireless communication platforms, including cognitive radio (CR) communication, 5G, and Wireless Local Area Network (WLAN) applications. A two-port Vivaldi antenna is designed using an FR4 substrate material with a dielectric constant of 4.4 and dimensions of 45.12 mm × 57.94 mm × 1.6 mm. This design is suitable for communication within a cognitive radio architecture. The antenna operates across multiple frequency bands, including the n79 band (4.4 GHz to 5 GHz) for 5G networks via port 1, and the 2.4 GHz band for Wi-Fi and Bluetooth communication via port 2. It achieves a return loss below -10 dB and a VSWR below 1.5 across the n79 band for 5G communication, and the 2.4 GHz band for WLAN applications.

Index Terms-Vivaldi antenna, cognitive radio, n79 band, 2.4 GHz Wi-Fi

I. INTRODUCTION

Cognitive Radio (CR) technology has emerged as a promising solution to address the spectrum scarcity issue in wireless communication systems. By enabling dynamic spectrum access and efficient utilization of the spectrum, CR systems can significantly enhance wireless performance and improve overall network capacity. A key component of CR systems is the cognitive radio antenna, which plays a crucial role in realizing the benefits of cognitive radio technology. A cognitive radio antenna is a specialized antenna system that integrates the principles of cognitive radio technology with advanced antenna design. Key characteristics of cognitive radio antennas include: Adaptability, Intelligent Sensing, Beamforming, and Cognitive Processing. Cognitive radio architecture has two primary stages sensing and communication. The project aims to propose cognitive radio antenna for communication stage of cognitive radio architecture. Ultra-wideband antenna is used for spectrum sensing stage of cognitive radio architecture. 5G communication frequency bands and WLAN frequency bands are used for communication stage of cognitive radio architecture. 5G Communication is the core of the fifth generation of wireless technology, enabling ultra-reliable, high-speed, low-latency data transmission. It is designed to meet the increasing demand for connectivity across devices, industries, and applications. 5G has three bands which are low-band, mid-band, and high-band or mmwave. Low-band has frequency range below 1 GHz. Mid-band has frequency range between 1 GHz to 6 GHz. It has three sub bands which are 2.5 GHz (n41) for Mobile broadband, urban coverage, 3.3–3.8 GHz (n77, n78) for Urban/suburban 5G, enterprise use, 4.4–5.0 GHz (n79) for High-capacity urban broadband. High-band has frequency range above 24 GHz. WLAN (Wireless Local Area Network) is a wireless communication technology that enables devices within a limited area, such as a home, office, or campus, to connect to a network and access the internet or communicate with each other. WLAN typically operates using standards defined by the IEEE 802.11 family, commonly known as Wi-Fi. The 2.4 GHz frequency band is a widely used range for short-range communication technologies like Bluetooth and Wi-Fi. Bluetooth is a short-range wireless technology standard used primarily for connecting devices and transferring data between them. It has frequency range of 2.4 GHz ISM (Industrial, Scientific, and Medical) 4 band (2.402 GHz to 2.480 GHz). It is used in data transfer between devices like smartphones and PCs. Wi-Fi in the 2.4 GHz band is a wireless local area network (WLAN) technology used for high-speed internet and data sharing over a broader range compared to Bluetooth. It has frequency range of 2.4 GHz ISM band (2.400 GHz to 2.4835 GHz). It is used in internet access for homes and offices. This project proposed Vivaldi antenna to operate in n79 band, and 2.4GHz Wi-Fi].

II. LITERATURE REVIEW

M. Kasiselvanathan et al.,[3] have analysed a multi-radio antenna system for Cognitive Radio (CR), NB MIMO (5G, WLAN), and UWB MIMO applications, integrating three independent antennas. The system includes a CR antenna (UWB sensing and two narrow-band communication antennas), a UWB MIMO antenna (two elements), and a NB MIMO antenna (two elements). The UWB antenna covers 3–12 GHz for CR sensing and UWB MIMO, while the NB antennas operate at 3.3, 3.5, 5, 5.5, and 8 GHz for CR and NB MIMO communication. Mutual coupling is minimized by orthogonally placing radiators with a parallel line stub. MIMO

performance is assessed through mutual coupling, envelope correlation coefficient, TARC, and channel capacity loss. [1]
Rifaqat Hussain et al.,[3] have analysed a novel integrated antenna system for cognitive radio (CR) applications, consisting of a compact 4-element reconfigurable annular slot-based MIMO antenna and a UWB sensing antenna. Designed on a single RO-4350 substrate (60×120×1.5 mm³), the MIMO antenna operates from 1.77 GHz to 2.51 GHz, while the UWB antenna covers 0.75–7.65 GHz. The system is suitable for CR-enabled wireless devices, with an envelope correlation coefficient (ECC) below 0.248 across the MIMO band. The maximum gain of the MIMO antenna is 3.2 dBi, and the efficiency reaches 81%. [2]

Amany A. Megahed et al.,[4] have analysed a compact four-port MIMO antenna system for 5G NR sub-6 GHz (n77/n78/n79) and 5 GHz WLAN, covering 3.2–5.75 GHz with good impedance matching. To improve isolation between elements, the antenna uses orthogonal orientations, a 0.3λo element spacing, and includes electromagnetic bandgap, defected ground structure, capacitive elements, and neutralization lines. The measured mutual coupling is reduced from −20 dB to −45 dB, and the envelope correlation coefficient, diversity gain, and radiation efficiency (90%) are enhanced. The antenna dimensions are 46 mm × 46 mm × 1.6 mm, with a measured gain of 6–9 dBi. Fabricated on an FR-4 substrate, the design reduces costs. EBG improves isolation to −65 dB, DGS to −60 dB, and CE to −40 dB, making it suitable for wideband 5G NR and WLAN applications. [3]

Soufian Lakrit et al.,[5] have analysed an integrated three-antenna structure for cognitive radio communication, covering 5G, WLAN, LTE, and ITU bands. The design includes a UWB antenna for spectrum monitoring (3.1–10.6 GHz) and two narrow-band antennas for communication. The UWB antenna, with a peak gain of 5.36 dBi at 10 GHz and 85% radiation efficiency, is connected to port 1. The first narrow-band antenna at port 2 covers 5–6 GHz (WLAN 5 GHz), while the second at port 3 supports dual bands (2.8–4.15 GHz and 7.7–11.2 GHz) for 5G, Wi-MAX, LTE, and ITU bands. The structure, built on an FR-4 substrate (28 × 37 × 1.6 mm³), shows good performance with transmission coefficients less than −13.5 dB across operating bands, verified through experimental testing. [4]

Arpan Desai et al.,[5] have analysed a flexible, transparent wideband four-element MIMO antenna is designed, using AgHT-4 conductive oxide and Melinex substrate to achieve optical transparency. The antenna features circular stub-loaded C-shaped resonators and an L-shaped partial ground plane, with a size of 0.33λ × 0.48λ at the lowest frequency. It covers a −10 dB impedance bandwidth of 2.21–6 GHz (92.32%) and offers high isolation (>15 dB). The maximum gain is 0.53 dBi, and efficiency is 41%, suitable for flexible applications. MIMO performance, including envelope correlation coefficient (ECC) and diversity gain, is satisfactory. Bending tests show stable performance, making this antenna ideal for IoT devices in 5G and WLAN bands, where integration on curved surfaces is needed. [5]

Xiongwen Zhao et al.,[3] have analysed a novel multi-mode frequency reconfigurable MIMO antenna design for cognitive radio applications, featuring two modified triangular monopole elements and a combination of varactor and PIN diodes. Three modes are supported by the antenna: UWB MIMO mode for communication, frequency reconfigurable MIMO mode for spectrum sensing, and UWB mode for spectrum sensing. In UWB mode, it covers 1–4.5 GHz, while frequency reconfigurability ranges from 0.9 to 2.6 GHz with varactor diode tuning. The compact antenna (120 × 60 × 1.5 mm³) achieves good MIMO performance with isolation of 12.5 dB and an ECC of less than 0.19. Measurement results validate the design. [6].

III. PROPOSED DESIGN OF VIVALDI ANTENNA

A co-planar broadband antenna, also known as a Vivaldi antenna, Vivaldi aerial, or tapered slot antenna, can be constructed from a printed circuit board, a solid sheet of metal, or a dielectric plate that has been metalized on one or both sides. A sector-shaped region or a direct coaxial connection can be used to terminate the feedline, which uses a microstrip line or coaxial cable to excite an open space.

Design Equations
Parameters required to design Vivaldi antenna

f_{min} = 2 GHz, f_{max} = 6 GHz, λ_{min}= 50 mm, λ_{max} = 200 mm

Length of substrate, L

$$L > \frac{\lambda_{\min} + \lambda_{\max}}{2} \tag{1}$$

$$L > \frac{200+50}{2}$$

L >125 mm

Width of substrate, W

$$W > \frac{\lambda_{\min} + \lambda_{\max}}{4} \tag{2}$$

$$w > \frac{200+50}{4}$$

W > 56.25 mm

Minimum mouth opening width, w_{min}

$$w_{\min} = \frac{\lambda_g}{f \cdot \varepsilon} \tag{3}$$

$w_{min} = 4.99$ mm

Maximum mouth opening width, w_{max}

$$w_{\max} = \frac{\lambda g}{2} \quad (4)$$

$w_{max} = 47.67$ mm

$$\lambda g = \frac{c}{f_{\min} \cdot \sqrt{\varepsilon}} \quad (5)$$

where λ_{max} and λ_{min} are maximum and minimum wavelength of minimum (f_{min}) and maximum (f_{max}) frequency of Vivaldi antenna. [7]

A. Various stages of vivaldi antenna for communication

Stage 1

Equations (1) to (5) are used to obtain the vivaldi antenna in Fig. 1.

Fig.1. 3D view of Vivaldi antenna

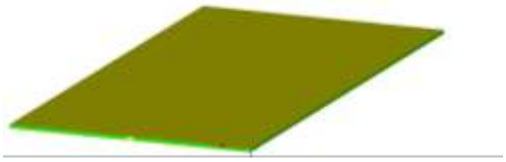

Fig. 2. Bottom view of Vivaldi antenna

The Vivaldi antenna in Fig. 1 resonates above -10 dB from 1 GHz to 6 GHz. It has a VSWR above 1.5 from 1 GHz to 6 GHz. Reduction in substrate size and patch size is done, which is shown in Fig. 3.

Stage 2

The Vivaldi antenna in Fig. 3 is obtained by reduction in size of substrate, and defected ground technique. Two ports are used for excitation.

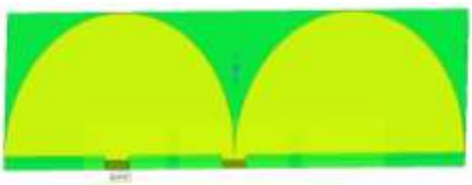

Fig. 3. 3D view of Vivaldi antenna without hexagonal slot

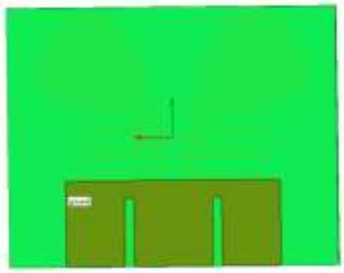

Fig. 4. Ground view of Vivaldi antenna without hexagonal slot

Port 1 and port 2 of the antenna are shown in Fig. 3; they resonate at 4.76 GHz and 2.4 GHz and have return losses of -23.4 dB and -7.51 dB, respectively. Ground structure is similar for further stages.

Stage 3

The Vivaldi antenna in stage 3 is obtained by taking hexagonal slots on both sides of the patch of the Vivaldi antenna in Fig. 3.

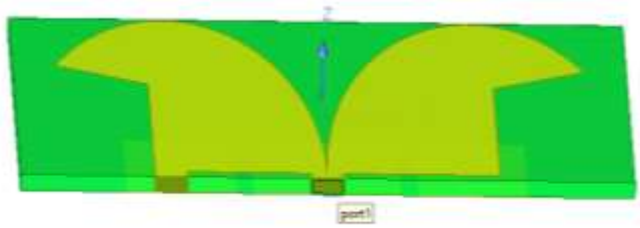

Fig. 5. 3D view of Vivaldi antenna with hexagonal slot

Port 1 of the antenna is shown in Fig. 5, which resonates at 4.79 GHz, and 2.53 GHz has a return loss of -18 dB and -17.6 dB, respectively. Port 2 resonates at 2.5 GHz and has a return loss of -11.2 dB.

Stage 4

A rectangular slot of dimension 10 mm x 2 mm is taken on both sides of the Vivaldi antenna patch in stage 3.

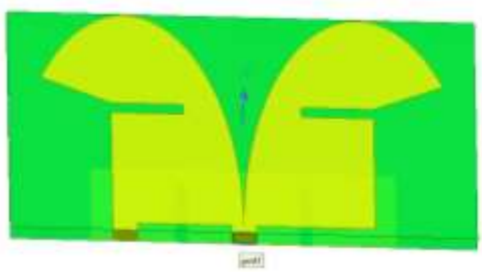

Fig. 6. 3D view of Vivaldi antenna with hexagonal and one rectangular slot

Port 1 of the antenna is shown in Fig. 6, which resonates at 4.71 GHz and 2.56 GHz, with return losses of -16 dB and -18 dB, respectively. Port 2 resonates at 2.57 GHz and has a return loss of -11.2 dB.

International Journal of Scientific Research & Engineering Trends
Volume 11, Issue 1, Jan-Feb-2025, ISSN (Online): 2395-566X

Stage 5

A rectangular slot of dimension 10 mm x 2 mm is taken on both sides of the Vivaldi antenna patch in stage 4.

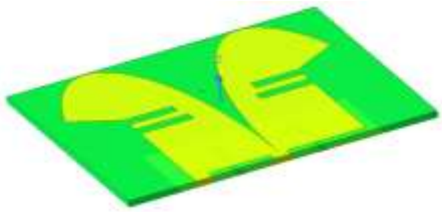

Fig. 7. 3D view of Vivaldi antenna with hexagonal and two rectangular slots

Port 1 of the antenna is shown in Fig. 7, which resonates at 4.72 GHz, and 2.55 GHz has a return loss of -20 dB and -19 dB, respectively. Port 2 resonates at 2.56 GHz and has a return loss of -11 dB.

Final Stage

Fig. 8. 3D view of Vivaldi antenna with hexagonal and three rectangular slots

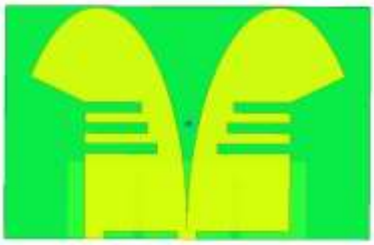

Fig. 9. Top view of Vivaldi antenna with hexagonal and three rectangular slots

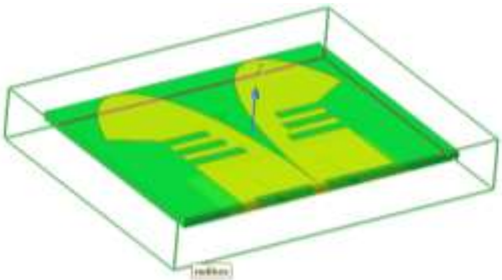

Fig. 10. 3D view of Cognitive Radio Vivaldi antenna with hexagonal and three rectangular slots

A rectangular slot of dimension 11.5 mm x 2 mm is taken on both sides of the Vivaldi antenna patch in stage 5. Port 1 of the antenna is shown in Fig. 8, which resonates at 4.82 GHz, and 2.54 GHz has a return loss of -26 dB and -18 dB, respectively. Port 2 resonates at 2.56 GHz and has a return loss of -11 dB. Fig. 9 and Fig. 10 show the front view and 3D view of the cognitive radio Vivaldi antenna, respectively.

The return loss of the Vivaldi antenna in Figure 1 is low. In Fig. 3, the Vivaldi antenna resonates at port 2 at 2.4 GHz with a return loss of -7.51 dB. At port 1, the Vivaldi antenna in Fig. 5, 6, and 7 resonates in dual band. Although the Vivaldi antenna in Fig. 8 has a large return loss at the n79 band, it likewise resonates at dual band in port 1. At port 1, it meets the 5G n79 band's frequency range. Its low VSWR and high return loss make it incompatible with the 2.4 GHz Wi-Fi frequency spectrum at port 2. The 5G n79 band and a small portion of the 2.4 GHz Wi-Fi spectrum are appropriate for cognitive radio communication applications using this antenna. In the future, slots will be added to enhance return loss and VSWR for 2.4 GHz and port 1 resonates at one band.

C. Comparison of results between various stages

Table 1 Results comparison of various stages

Stages/parameters		Resonating frequencies	Return loss
First	Port1	2GHz to 6GHz	>-10dB
Second	Port1	4.76GHz	-23.4dB
	Port2	2.4GHz	-7.51dB
Third	Port1	4.79GHz, 2.53 GHz	-18dB, -17.6 dB
	Port2	2.5 GHz	-11.2dB
Fourth	Port1	4.71GHz, 2.56GHz	-16dB, -18dB
	Port2	2.57GHz	-11.2dB
Fifth	Port1	4.72 GHz, 2.55 GHz	-20dB, -19dB
	Port2	2.56 GHz	-11 dB
Final	Port1	4.82 GHz, 2.54 GHz	-26 dB, -18 dB
	Port2	2.56 GHz	-11 dB

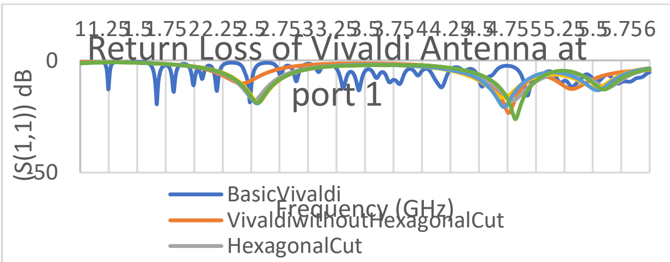

Fig. 11. S(1,1) of Vivaldi antenna from first stage to final stage

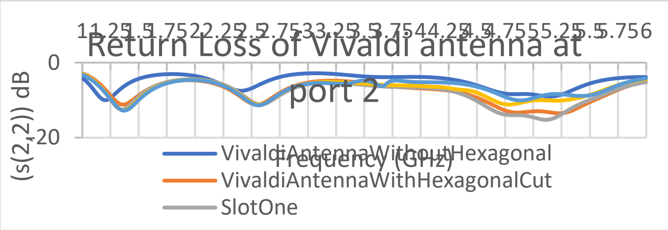

Fig. 12. S(2,2) of Vivaldi antenna from second stage to final stage

Return loss of the Vivaldi antenna at port 1 and port 2 for various stages is shown in Fig. 11 and Fig. 12, respectively.

IV. RESULTS

1. Performance Metrics

Return Loss is a measurement of the amount of signal power that is reflected back toward the source instead of being delivered to a load.

$$RL(\text{dB}) = -20 \log|\Gamma|$$

VSWR is a measurement of how well radio frequency power is transmitted through a transmission line to a load.

$$VSWR = \frac{1 + |\Gamma|}{1 - |\Gamma|}$$

Radiation pattern of graphical representation of the spatial distribution of the radiated power emitted by an antenna. Co-polarization is the antenna's radiation in desired directions. Cross-polarization is the antenna's radiation in the unwanted directions

2. Simulation Results

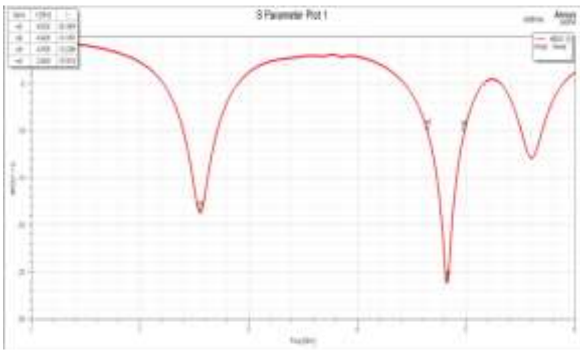

Fig. 13. Return loss of CR vivaldi antenna at port 1

Port 1 of the CR antenna resonates at 4.82 GHz with a return loss of -26.18 dB. It has a return loss below -10 dB from 4.64 GHz to 4.97 GHz, which is shown in Fig. 13.

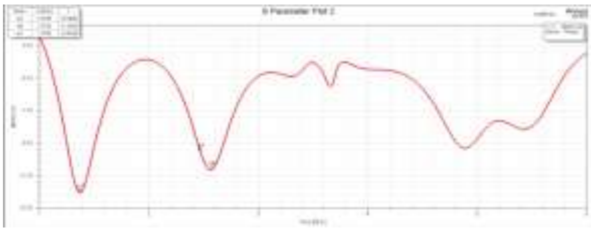

Fig. 14. Return loss of CR vivaldi antenna at port 2

Port 2 of the CR antenna resonates at 1.37 GHz and 2.56 GHz with a return loss of -12.81 dB and -11.39 dB, respectively. It has a return loss below -10 dB at 2.47 GHz, which is shown in Fig. 14.

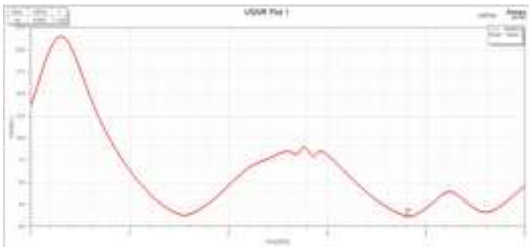

Fig. 15. VSWR of CR vivaldi antenna at port 1

Port 1 of the CR antenna resonates at 4.81 GHz with a VSWR of 1.11. It has a VSWR below 2 from 4.64 GHz to 4.97 GHz, which is shown in Fig. 15.

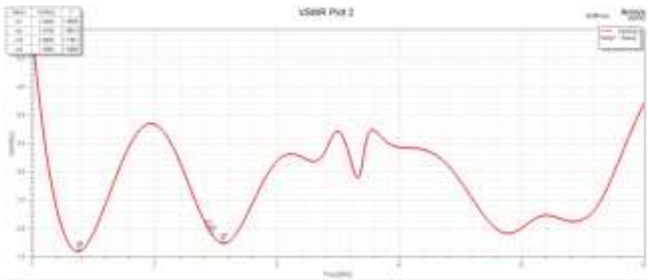

Fig. 16. VSWR of CR vivaldi antenna at port 2

Port 2 of the CR antenna resonates at 1.38 GHz and 2.56 GHz with a VSWR of 1.59 and 1.7, respectively. It has a VSWR below 2 at 2.47 GHz, which is shown in Fig. 16.

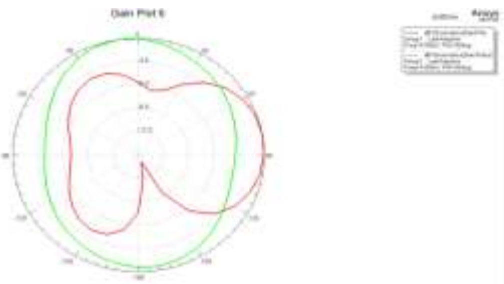

Fig. 17. Radiation pattern in H-plane of CR Vivaldi antenna at 4.8GHz

In Fig. 17, the red curve and green curve indicate co-polarization and cross-polarization in the H-plane, respectively, at 4.8 GHz of port 1.

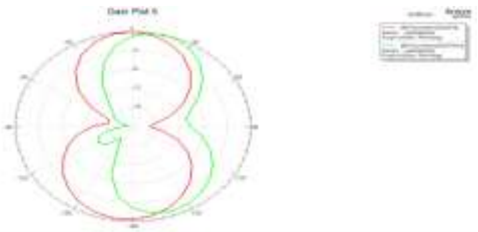

Fig. 18. Radiation pattern in E-plane of CR Vivaldi antenna at 4.8GHz

In Fig. 18, the red curve and green curve indicate cross-polarization and co-polarization in the E-plane, respectively, at 4.8 GHz of port 2.

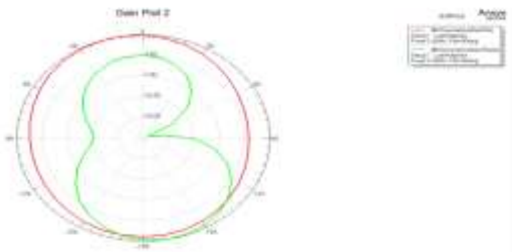

Fig. 19. Radiation pattern in H-plane of CR Vivaldi antenna at 2.4GHz

In Fig. 19, the red curve and green curve indicate co-polarization and cross-polarization in the H-plane, respectively, at 2.4 GHz of port 1.

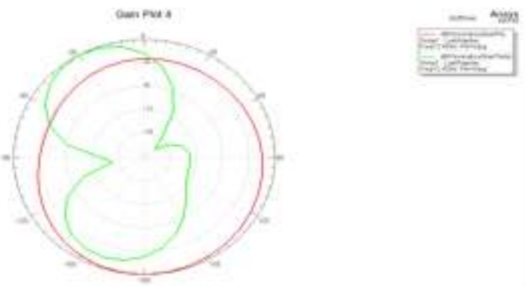

Fig. 20. Radiation pattern in E-plane of CR Vivaldi antenna at 2.4GHz

In Fig. 20, the red curve and green curve indicate cross-polarization and co-polarization in the E-plane, respectively, at 2.4 GHz of port 2.

V. CONCLUSION

The proposed cognitive radio antenna supports multiple applications including cognitive radio, 5G and WLAN applications. It is designed using FR-4 substrate material in Ansys 2023/R2 High Frequency Structure Simulation (HFSS) software with small physical dimension 45.12 mm × 57.94 mm × 1.6 mm as compared to literature studies. Return loss and VSWR of -26 dB and 1.11 is achieved at n79 band of 4.8 GHz for 5G communication. Return loss and VSWR of -10.28 dB and 1.8 is achieved at 2.47 GHz Wi-Fi for WLAN. The proposed antenna has bandwidth of 336 MHz for n79 band 5G communication. In the future, we'll design the spectrum sensing antenna on the proposed substrate and improve return loss and VSWR for 2.4 GHz Wi-Fi.

REFERENCES

1. M. Kasiselvanathana, Prabhu P, L. Rajac, and Sivaprasad Lebaka, “A multi-radio antenna system for Cognitive Radio (CR), 5G, WLAN and UWB MIMO applications”, AEU- International Journal of Electronics and Communications,13 May 2024, https://doi.org/10.1016/j.aeue.2024.155315
2. Rifaqat Hussain, Mohammad, S. Sharawi and Atif Shamim, “An Integrated 4-element Slot-Based MIMO and an UWB Sensing Antenna System for CR Platforms”, IEEE Access, 2023, doi: 10.1109/TAP.2017.2781220
3. Amany a. megahed, Mohamed abdelazim, Ehab H. Abdelhay and Heba Y. M. Soliman,“Sub-6 GHz Highly Isolated Wideband MIMO Antenna Arrays”, IEEE Access, Volume 10, 2022, doi:10.1109/ACCESS.2022.3150278
4. Soufian Lakrit, Anveshkumar Nella, and Ch Murali Krishna, “An integrated three-antenna structure for 5G, WLAN, LTE and ITU band cognitive radio communication”, AEU- International Journal of Electronics and Communications, 30 July 2021, https://doi.org/10.1016/j.aeue.2021.153906
5. Arpan desai, Merih palandoken, Jayshri kulkarni and Gangil byun, “Wideband Flexible/Transparent Connected-Ground MIMO Antennas for Sub-6 GHz 5G and WLAN Applications”, IEEE Access, Volume 9, 2021, doi:10.1109/ACCESS.2021.3123366
6. Xiongwen Zhao, Sharjeel Riaz, and Suiyan Geng, “A Reconfigurable MIMO/UWB MIMO Antenna for Cognitive Radio Applications”, IEEE Access, Volume 7,2019, doi:10.1109/ACCESS.2019.2909810
7. M. M. Rana, R. Khanom and M. M. Rahman, "Design and Analysis of Vivaldi Antennas," 2018 International Conference on Innovation in Engineering and Technology (ICIET), Dhaka, Bangladesh, 2018, pp. 1-5, doi: 10.1109/CIET.2018.8660793